An Investigation of Stable Waves along a Velocity Shear Boundary in a Two-Layer Sea with a Geostrophic Flow Regime[1]

Alyn C. Duxbury

Bingham Oceanographic Laboratory
Yale University

ABSTRACT

The physical characteristics of a certain class of stable perturbations in an idealized oceanic current regime are investigated theoretically and compared with some observed features of the Gulf Stream. The mathematical model envisages an idealized two-layer fluid with a deep lower layer that remains essentially in static balance. The upper layer, when in equilibrium, is characterized by a region of uniform geostrophically balanced current (hence of nonuniform thickness); adjoining this is a second region of uniform thickness that is at rest. Under disturbed conditions, the kinematic (shear) boundary that delineates the two regions is subject to transverse excursions (or meanderings) associated with the vertical displacement of the interface between the upper and lower layers.

Only those disturbances with energy confined to the region of the shear boundary have been investigated in this study. Two classes of shear boundary waves occur: inertio-gravitational and quasi-geostrophic. Stable modes for both classes are found to exist over the range 0.1 to 10 in the internal Froude number. However, the range of wave lengths for stable waves is dependent upon the internal Froude number. Moreover, it is only those flow-regimes for which the internal Froude number exceeds unity that *stationary meanders* in the stream are possible. Although the free perturbations are dynamically stable, they are of dispersive character (the phase-speed being wave-length dependent). This implies that a general disturbance of the current boundary, as represented by a combination of many different modes, cannot remain in a permanent form. This aspect, together with the possibility of resonant coupling with the atmosphere, can lead to a growth, with time, of the disturbance and is suggestive of Gulf Stream meanders. The analysis shows that the quasi-geostrophic modes have characteristics that are most consistent with observed meanders of the Gulf Stream.

Introduction. A simplified model representative of a geostrophically balanced flow-regime in the ocean has been analyzed dynamically to determine under

[1] This study was conducted in partial fulfillment of the requirements for a Ph. D. degree at the Agricultural and Mechanical College of Texas under Professor Robert O. Reid, Department of Oceanography and Meteorology.

what conditions stable shear waves can exist along the edge of a stream. The model chosen for this analysis is identical to the one proposed by Iwata (1961); however, there are some important differences in the approach and results in the present study.

The problem of determining the governing factors that cause the velocity shear boundaries of oceanic streams to meander (such as the Gulf Stream and Kuroshio) has been investigated before. Haurwitz and Panofsky (1950), using perturbation techniques, investigated a barotrophic model of the Gulf Stream. Their investigation centered upon the role played by cross-stream velocity profiles in determining the stability or instability of the shear boundary waves. They determined that the proximity of the velocity shear boundary to the edge of the continental slope controlled the stability of the meanders. Even though their analysis incorporated realistic cross-stream velocity profiles, their omission of density stratification leaves some doubt as to the applicability of their results to the Stream.

Stommel (1953) investigated the stability of a broad surface current for a two-layer system. In his analysis, the current was considered to be uniform and of infinite width. The basic flow was considered to be representative of a geostrophic equilibrium, which requires that the depth of the upper layer increase to the right of the flow (in the northern hemisphere). However, in his analysis, Stommel treated the upper layer depth as uniform. His results indicate that, for $F^2 = V^2/g'D > 1$ (supercritical internal Froude number), some perturbations are unstable, depending upon their wave length. Unfortunately, his approximation of uniform depth implies that the results are restricted to values of $F^2 \ll 1$. Hence the instability predicted by theory transcends the conditions of its applicability.

The object of the present study is to show that stable waves can exist in the presence of a velocity shear boundary for conditions of F^2 greater than, as well as less than, unity. The character of these stable boundary waves and the range of wave lengths for which these exist is studied in some detail.

List of Symbols

B $(\varrho H + \varrho' H')/\varrho'$, eq. (17).
b Turning point for Z_1, eq. (60).
c Phase-speed (σ/k).
D, D_0 Equilibrium depth of upper layer for $y < 0$ and $y = 0$, respectively.
D_j Equilibrium depth for region 1 or 2.
E $W/2W'$, eq. (84).
F Internal Froude number $(U/\sqrt{g'D_0})$.
f Coriolis parameter.
G Transform of Z_1, eq. (53).
g Gravity.

g' Effective gravity for internal disturbances,

$$g' = (\Delta\varrho/\varrho')\, g.$$

H, H' Thickness of the disturbed upper and lower layers, respectively.
H_j Thickness of disturbed upper layer for region 1 or 2.
h_j Perturbation of vertical thickness for region 1 or 2.
i $\sqrt{-1}$.
j Subscript denoting region 1 or 2; $y<0, y>0$.
K A parameter with dimensions $[L^{-1}]$, eq. (49).
K_n Modified Bessel function.
k Longitudinal wave number.
M Exponential parameter, eqs. (68) and (77).
m $m^2 = -M^2$.
N Variable wave number of eq. (55).
n Integer index (0, 1, 2, . . .), indicating wave mode.
P, P' Pressure in upper and lower layer, respectively.
P_a Atmospheric pressure.
P'_b Pressure at bottom.
p Integer index (0, 1, 2, . . .).
Q, Q' Quadratic operator for upper and lower layer, respectively.
s Slope of equilibrium interface, region 1 ($y<0$).
T Wave period.
t Time.
U Basic state velocity of upper layer, region 1 ($y<0$).
u, v x- and y-directed velocity, respectively.
$\hat{u}_j, \hat{v}_j$ x- and y-directed perturbation of velocity for region 1 or 2, respectively.
V_j Basic state velocity for region 1 or 2 (U, 0, respectively).
W Function of α and z, defined by (69) and (64).
X_j, Y_j x- and y-dependent amplitudes of the x- and y-directed perturbation of velocities respectively.
x, y x- and y-coordinates (x taken in direction of basic flow).
Z_j y-dependent amplitude of the perturbation of vertical thickness.
z Transformation variable, eq. (54); and also z-coordinate.
z_0 Transformation variable evaluated at $y = 0$, eq. (70).

α A characteristic parameter, eq. (62).
$\Gamma(x)$ Gamma function, $\Gamma(x+1) = x\Gamma(x)$.
γ Relative frequency, ω/f.
η Displacement of vortex sheet.
λ Wave length.
μ Relative wave length, kU/f.
ξ Energy density (on a per-unit-area basis).
ϱ, ϱ' Density of upper and lower water layer, respectively.

σ Wave frequency, $2\pi/T$.
Φ Kummer function, eq. (63).
φ Latitude.
Ψ Tricomi function, eq. (64).
ψ $d\Gamma(\alpha)/d\alpha$.
Ω Earth's angular velocity.
ω_j Symbolizes ω, σ ($j = 1, 2$, respectively).
ω $\sigma - kU$.
ζ Vorticity.

THEORY

1. *Choice of a Model.* As in Stommel's analysis, a uniform geostrophically balanced flow of the upper layer in a two-layer system is considered. However, it is recognized that even in the abstraction of the model, the current cannot be of indefinite width in both directions. The following three possibilities exist in regard to the termination of the uniform flow-regime on the left side of the current: (i) parallel to the flow there exists a rigid lateral boundary at which D (depth of upper flowing water) has some specific value D_0; (ii) a free boundary occurs at which $D = 0$ (i. e. the interface between layers terminate at the free surface of the fluid); and (iii) the moving layer terminates abruptly at the lateral junction of the moving layer and a stationary layer of the same density.

(i) The first of these geometrical configurations was investigated by Reid and Duxbury (1960) in an attempt to extend the Stommel theory to suitably large values of the internal Froude number by making due allowance for the nonuniform layer depth. The results of that study indicate that the perturbations are stable for all values of F^2. This is consistent with the results of Haurwitz and Panofsky (1950) for a similar case in which the velocity shear occurs at a rigid boundary (see Introduction).

(ii) The second possibility is a special case of (i) in which the edge-wave analysis by Reid (1958) is pertinent. As in case (i), it is shown that all free disturbances of regular behavior at the free boundary are dynamically stable. However, note that there exists no allowance for lateral transfer of energy across the lateral boundary in either case.

(iii) The third geometrical configuration comes somewhat closer to reality and is the one presented in this analysis. This model (Figs. 1–3) allows for a sharp boundary of the current and at the same time retains the two-layer system throughout. Thus the combined influence of stratification and lateral shear of the flow is incorporated and allowed to enter into the dynamic analysis in its true light.

It should be borne in mind that the present analysis does not attempt to take into account a continuously varying lateral distribution of velocity for the basic flow. Instead, the attention is focused on the limiting case of an abrupt change in the velocity of the basic flow.

The present model is not developed specifically for the Gulf Stream, Kuroshio, or any other major surface current, but the highly idealized system analyzed here can be likened to such currents. Throughout the text, the Gulf Stream is referred to as a prototype of the model, primarily as a matter of convenience in determining whether reasonable results could be obtained from the model.

2. *Formulation of the Problem.* A diagram of the two-layer model is shown in Figs. 1–3. The upper and lower layers are presumed to be of uniform density, ϱ and ϱ', respectively, where $\varrho' > \varrho$. For convenience in notation, all variables with prime relate to the lower layer. The instantaneous thicknesses of the two layers are denoted by H and H'. In general, these quantities are functions of x, y, and t, the horizontal position coordinates, and time, respectively. The x-axis is taken in the direction of uniform mean flow, U, which exists in region 1 of the upper layer. The plane, $y = 0$, is identified with the equilibrium state of the kinematic shear boundary between the flowing and stationary parts of the upper layer. The subscripts 1 and 2 are employed to denote the regions on either side of this boundary, $y < 0$ and $y > 0$, respectively.

The important assumptions employed in the development are as follows:

(A) The pressure distribution in the vertical direction is given by the hydrostatic relation;

(B) The Coriolis parameter (vertical component of the earth's vorticity) is considered constant;

(C) The curvature of the earth is neglected, implying that the gravity vector is everywhere normal to the planes Z = constant;

(D) Attention is confined to baroclinic (internal) disturbances in a system with $D'_0 \rangle\rangle D_0$;

(E) The domain of the fluid is considered unbounded with respect to the x- and y-coordinates (except for the internal kinematic boundary);

(F) The disturbances of the system from the state of equilibrium are considered to be suitably small;

(G) The equilibrium state is considered to be representative of a state of geostrophic balance, with the lower layer at rest;

(H) Fluid friction and external driving forces are ignored.

The basic equations of motion for free disturbances of the upper layer, referred to a cartesian coordinate system rotating with the earth, are:

$$\frac{du}{dt} - fv + \frac{1}{\varrho}\frac{\partial P}{\partial x} = 0, \tag{1}$$

$$\frac{dv}{dt} + fu + \frac{1}{\varrho}\frac{\partial P}{\partial y} = 0, \tag{2}$$

where $d/dt = \partial/\partial t + u(\partial/\partial x) + v(\partial/\partial y)$, and the pressure, P, is considered to

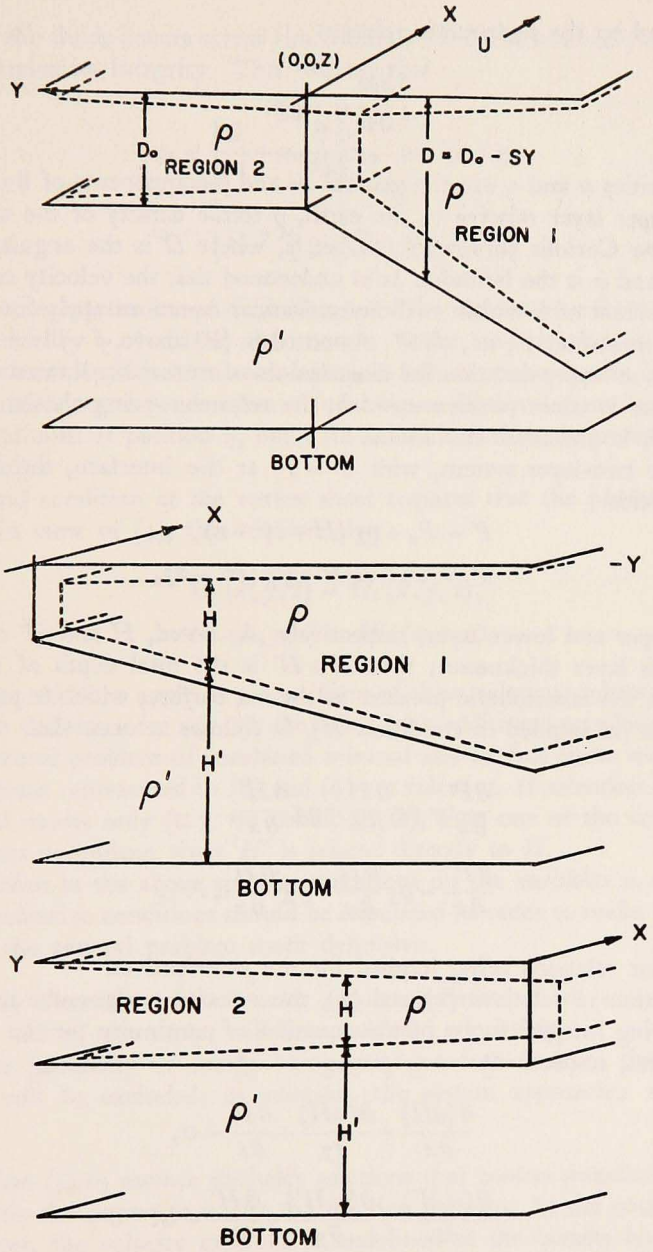

Figures 1, 2, and 3 (top to bottom). Diagram of the two-layer model: the equilibrium state is indicated by full lines, the disturbed state by dashed lines. For the equilibrium state, the upper layer of region 1 has a uniform geostrophically balanced flow, U, while region 2 is at rest. The plane $y = 0$ represents a velocity shear boundary (vortex sheet) in the undisturbed state.

be governed by the hydrostatic relation

$$\frac{\partial P}{\partial z} = -\varrho g. \tag{3}$$

The quantities u and v are the general x- and y-components of fluid velocity for the upper layer relative to the earth, ϱ is the density of the same layer, and f is the Coriolis parameter ($2\Omega \sin \varphi$, where Ω is the angular speed of the earth and φ is the latitude). It is understood that the velocity components are independent of z within each layer. Similar equations apply for the lower layer in terms of u', v', w', ϱ', P'. As noted in (B) above, f will be considered constant as an approximation for disturbances of reasonably limited scale. The z-coordinate is taken positive upward, the reference being chosen at the sea bed, which is presumed horizontal.

For the two-layer system, with $P = P'$ at the interface, the hydrostatic relation yields

$$\begin{aligned} P &= P_a + \varrho g (H + H' - z), \\ P' &= P_a + \varrho g H + \varrho' g (H' - z), \end{aligned} \tag{4}$$

for the upper and lower layer, respectively. As noted, H and H' are the instantaneous layer thicknesses; thus $H + H'$ is the total depth of fluid. The term P_a is the atmospheric pressure at the sea surface, which is presumed to be uniform (as implied in condition H). It follows at once that

$$\begin{aligned} \frac{\partial P}{\partial x} &= \varrho g \frac{\partial H}{\partial x} + \varrho g \frac{\partial H'}{\partial x}, \ldots, \\ \frac{\partial P'}{\partial x} &= \varrho g \frac{\partial H}{\partial x} + \varrho' g \frac{\partial H'}{\partial x}, \ldots, \end{aligned} \tag{5}$$

with similar relations being implied for the y-derivatives.

In addition to relations (1) and (2), the velocity components must satisfy the following integral forms of the equation of continuity for the upper and lower layers, respectively:

$$\frac{\partial (uH)}{\partial x} + \frac{\partial (vH)}{\partial y} + \frac{\partial H}{\partial t} = 0, \tag{6}$$

$$\frac{\partial (u'H')}{\partial x} + \frac{\partial (v'H')}{\partial y} + \frac{\partial H'}{\partial t} = 0. \tag{7}$$

The position of the vertical vortex sheet, which represents the internal boundary of the basic flow in the upper layer, is subject to transverse excursions associated with internal disturbances. However, it is presumed that no lateral

mixing of the fluids occurs across this interface; i. e. the boundary of the basic flow maintains its integrity. This implies that

$$v_1 = \left\{\frac{\partial}{\partial t} + u_1 \frac{\partial}{\partial x}\right\}\eta, \quad \text{at} \quad y = \eta,$$
$$v_2 = \left\{\frac{\partial}{\partial t} + u_2 \frac{\partial}{\partial x}\right\}\eta, \quad \text{at} \quad y = \eta, \tag{8}$$

where η represents the lateral displacement of the vortex sheet from its equilibrium position ($y = 0$). Since the motion under investigation is considered independent of depth (within each layer), it follows that η is also independent of depth and hence depends upon x and t alone. Both relations in (8) pertain to the conditions at position η, but with u and v evaluated for regions 1 and 2, separately.

A second condition at the vortex sheet requires that the pressure be continuous. In view of (4), this requires that

$$H_1(x, y, t) = H_2(x, y, t),$$
$$H'_1(x, y, t) = H'_2(x, y, t), \tag{9}$$

where both relations apply at $y = \eta$. One of these relations represents merely an implicit definition for $\eta(x, t)$; the other is an additional coupling condition. In the general problem of combined internal and surface-wave modes, all of the conditions represented in (8) and (9) are relevant. If attention is confined to internal modes only (e. g. by condition D), then one of the conditions in (9) becomes redundant, since H' is related directly to H.

In addition to the above specific conditions on the variables u, v, H, etc., certain qualitative conditions should be stipulated in order to make the formulation of the general problem more definitive:

(I) Only those disturbances with regular behavior at all x and y within regions 1 and 2, separately, will be considered admissible;

(J) The possibility of energy being propagated to or from the system at $y = \pm\infty$ will be excluded; in addition, the system approaches equilibrium there.

Condition (I) in essence excludes solutions that possess singularities at any point within the region to which the solution pertains. At the position of the vortex sheet, the velocity gradient is undefined at the outset; however, the condition of regularity with respect to the quantities u, v, and H should be required here. Condition (J) restricts the scope of the study to disturbances whose energy is confined to a finite region in the vicinity of the vortex sheet, in the same sense that the energy of the Kelvin tide-wave is confined to the

region of a fixed boundary. In essence, it is the wave-guide characteristics of the stream boundary that are of concern in this study.

3. *Equilibrium State.* Clearly, if the lower layer is at rest, as presumed for the equilibrium state, then from (5), with $\partial P'/\partial x = 0$, it follows that

$$\frac{\partial H'}{\partial x} = \frac{-\varrho}{\varrho'}\frac{\partial H}{\partial x}. \tag{10}$$

Accordingly,

$$\frac{\partial P}{\partial x} = \varrho g \frac{\Delta\varrho}{\varrho'}\frac{\partial H}{\partial x}, \cdots, \tag{11}$$

with a similar relation implied for the y-derivative, where $\Delta\varrho = \varrho' - \varrho$.

A simple steady-state regime for the upper layer, satisfying (1), (2), and (11), is that for which

$$u = V(y), \qquad v = 0, \qquad H = D(y), \tag{12}$$

where the functions $D(y)$ and $V(y)$ are related by the geostrophic relation

$$fV + g'\frac{dD}{dy} = 0, \tag{13}$$

where g' is the effective gravity, $g(\varrho' - \varrho)/\varrho'$. This also satisfies continuity within the limitations imposed by (B). The form selected for $V(y)$ in the present model is the step function

$$V(y) = \begin{cases} U, & y < 0, \\ 0, & y > 0, \end{cases} \tag{14}$$

where U is a constant. Thus (13) yields

$$D(y) = \begin{cases} D_0 - sy, & y < 0, \\ D_0, & y > 0, \end{cases} \tag{15}$$

where

$$s = \frac{fU}{g'} \tag{16}$$

is a constant slope of the interface and D_0 is the equilibrium depth of the upper layer at $y = 0$. It should be evident that the boundary conditions are satisfied automatically.

There is an inconsistency in the model that deserves some comment. This pertains to the conflict of relation (15) with the earlier stipulation of finite total depth of the fluid. It is evident that, for a total equilibrium depth or $D_0 + D'_0$ at $y = 0$, the width of the stream is limited to the value D'_0/s. It is

supposed in the subsequent development that D_0 can be chosen arbitrarily large so that the stipulation of (15) holds for the effective range of y that is pertinent to a given localized disturbance. This point is demonstrated later in the work on page 274.

4. *Transformation of the Basic Equations.* By employing relations (5) and the definition

$$B \equiv (\varrho H+\varrho' H')/\varrho', \tag{17}$$

it is readily shown that the equations of motion for the upper and lower layers can be rendered into the form

$$\begin{aligned} Q\{u\} - fv + g'\frac{\partial H}{\partial x} + g\frac{\partial B}{\partial x} &= 0, \\ Q\{v\} + fu + g'\frac{\partial H}{\partial y} + g\frac{\partial B}{\partial y} &= 0, \end{aligned} \tag{18a}$$

and

$$\begin{aligned} Q'\{u'\} - fv' + g\frac{\partial B}{\partial x} &= 0, \\ Q'\{v'\} + fu' + g\frac{\partial B}{\partial y} &= 0. \end{aligned} \tag{18b}$$

The symbols Q and Q' are introduced to designate the operations

$$\begin{aligned} Q &= \left\{\frac{\partial}{\partial t} + u\frac{\partial}{\partial x} + v\frac{\partial}{\partial y}\right\}, \\ Q' &= \left\{\frac{\partial}{\partial t} + u'\frac{\partial}{\partial x} + v'\frac{\partial}{\partial y}\right\}. \end{aligned} \tag{19}$$

A useful alternative continuity relation involving B is obtained from the sum of (6) and (7) after multiplying these by ϱ and ϱ', respectively:

$$\frac{\partial}{\partial x}(\varrho Hu + \varrho' H'u') + \frac{\partial}{\partial y}(\varrho Hv + \varrho' H'v') + \frac{\partial(\varrho' B)}{\partial t} = 0. \tag{20}$$

It is apparent from the definition (17) that $\varrho' B$ is simply the total mass of fluid in a column of unit cross-sectional area extending from the sea bed to the free surface. Hence (20) is simply a statement of the mass budget for the total column. Moreover, in view of (4), the bottom pressure (at $z = 0$) is

$$P'_b = P_a + \varrho' g B. \tag{21}$$

Thus B can be regarded as an equivalent depth in the sense that it is a measure of the pressure at the sea bed, for a given value of P_a.

The above relations govern both barotropic and baroclinic type disturbances of the system. The baroclinic perturbations are characterized by a nearly invariant value of B and a nearly zero net mass transport for the total depth. These conditions are consistent with (20). Thus the order of magnitude of u' and v' are

$$u' \sim \frac{-H}{H'}(u - V), \qquad v' \sim \frac{-H}{H'} v \tag{22}$$

for the baroclinic disturbances. Accordingly, it follows from (18a) and (18b) that

$$\begin{aligned} g\frac{\partial B}{\partial x} &\sim -g'\frac{H}{(H+H')}\frac{\partial(H-D)}{\partial x}, \\ g\frac{\partial B}{\partial y} &\sim -g'\frac{H}{(H+H')}\frac{\partial(H-D)}{\partial y}. \end{aligned} \tag{23}$$

Hence for the condition of a relatively thin upper layer ($H/H' \ll 1$), such as generally exists in the ocean, it is justifiable to neglect the gradient of B in (18a).

Thus, for baroclinic disturbances in a system with a deep lower layer, the governing equations for u, v, and H are

$$Q\{u\} - fv + g'\frac{\partial H}{\partial x} = 0, \tag{24}$$

$$Q\{v\} + fu + g'\frac{\partial H}{\partial y} = 0, \tag{25}$$

$$\frac{\partial H}{\partial t} + \frac{\partial(uH)}{\partial x} + \frac{\partial(vH)}{\partial y} = 0. \tag{26}$$

The solutions appropriate to regions 1 and 2 must be matched such that (8) and (9) are satisfied. However, since H' is determined by H for the condition of constant B, only one of the relations in (9) is pertinent. Moreover, since the other relation is simply an implicit equation for η, it follows that condition (8) can be expressed in the form

$$Q_1\{H_1 - H_2\} = 0, \tag{27}$$

$$Q_2\{H_1 - H_2\} = 0, \tag{28}$$

at $(H_1 - H_2) = 0$, where the operators Q_1 and Q_2 are given by (19), with the particular values of u and v appropriate to regions 1 and 2, respectively.

5. *The Perturbation Equations.* Relations (24) to (28) are nonlinear with respect to the dependent variables u, v, and H. However, if the departures

from the state of equilibrium are suitably small, then the linear approximations of these relations in terms of the perturbation variables are applicable.

In this connection, it is convenient to introduce the notations

$$\left.\begin{aligned} u_j &= V_j + \hat{u}_j, \\ v_j &= 0 + \hat{v}_j, \\ H_j &= D_j + h_j, \end{aligned}\right\} \tag{29}$$

where the subscript j (= 1, 2) denotes the region of the upper layer to which the particular set of functions pertains, and where $\hat{u}_j$, $\hat{v}_j$, and h_j represent perturbations superimposed on the basic state. The terms V_j and D_j designate the quantities

$$\begin{aligned} V_j &= U, 0 \\ D_j &= D_0 - sy, D_0 \end{aligned} \tag{30}$$

for j = 1, 2, respectively, where s is given by (16). These correspond to the equilibrium state for the two regions, although it is emphasized that the restriction on y implied in relations (14) and (15) does not apply to V_j and D_j.

Specifically, the set of functions $\hat{u}_j$, $\hat{v}_j$, and h_j for j = 1 have physical meaning for $y < \eta(x, t)$, and those corresponding to j = 2 have physical meaning for $y > \eta(x, t)$, where η is the position of the vortex sheet in the disturbed state. For undisturbed conditions the perturbations $\hat{u}_j$, $\hat{v}_j$, h_j, and η vanish, hence (30) is consistent with (14) and (15) under these conditions. The use of the double-value reference state near y = 0, as implied by (29) and (30) for disturbed conditions, is simply an artifice that allows $\hat{u}_j$, $\hat{v}_j$, and h_j to be continuous functions at and near y = 0. Any discontinuities in the system are confined to the position of the vortex sheet at $y = \eta(x, t)$, where the two sets of functions must be taken such that the kinematic boundary conditions are satisfied.

The perturbations $\hat{u}_j$, $\hat{v}_j$, and h_j for both regions are to be regarded as functions of x, y, and t in general. However, it is supposed that the magnitudes of these quantities are small for any x, y, and t, in the sense that

$$|\hat{u}_j|, \quad |\hat{v}_j| \ll \sqrt{g' D_0}, \quad \text{and} \quad |h_j| \ll D_0. \tag{31}$$

Under these conditions, the differential relations (24) to (26) can be reduced to the following linear system when second order terms, namely those involving products of the perturbation variables, are neglected:

$$\left(\frac{\partial}{\partial t} + V_j \frac{\partial}{\partial x}\right)\hat{u}_j - f\hat{v}_j + g' \frac{\partial h_j}{\partial x} = 0, \tag{32}$$

$$\left(\frac{\partial}{\partial t} + V_j \frac{\partial}{\partial x}\right)\hat{v}_j + f\hat{u}_j + g' \frac{\partial h_j}{\partial y} = 0, \tag{33}$$

$$\left(\frac{\partial}{\partial t}+V_j\frac{\partial}{\partial x}\right)h_j+\frac{\partial}{\partial x}(D_j\hat{u}_j)+\frac{\partial}{\partial y}(D_j\hat{v}_j)=0. \tag{34}$$

For region 2, these equations have a particularly simple form, since V_2 vanishes and D_2 has the constant value D_0.

The lateral excursion of the boundary can be expressed in terms of the variables h_1 and h_2 by means of the condition $H_1 = H_2$ at $y = \eta$. Use of (29) and (30) gives

$$\eta = (h_1 - h_2)/s, \tag{35}$$

where h_1 and h_2 are evaluated at $y = \eta$. However, if $h_1 = h_2$ is expressed by a Taylor series expansion about $y = 0$ and if second order terms are neglected, it follows that the first approximation for η, which is consistent with relations (32) to (35), is simply (35) with $(h_1 - h_2)$ evaluated at $y = 0$.

The latter relation allows the evaluation of $\eta(x, t)$ if the functions $h_j(x, y, t)$ are known, but it does not impose any condition on the functions $\hat{u}_j$, $\hat{v}_j$, and h_j. The coupling of the perturbations for regions 1 and 2 is provided by conditions (27) and (28). An expansion of the functions in these relations about $y = 0$, with subsequent neglect of second order terms, yields the following linear boundary conditions at $y = 0$:

$$\left(\frac{\partial}{\partial t}+V_j\frac{\partial}{\partial x}\right)(h_1 - h_2) - s\hat{v}_j = 0 \tag{36}$$

for $j = 1$ and 2. With (35) and the definition of V_j, relations (36) can be expressed in the alternative form

$$\begin{aligned}(\hat{v}_1 - \hat{v}_2) &= U\frac{\partial \eta}{\partial x},\\ \hat{v}_2 &= \frac{\partial \eta}{\partial t},\end{aligned} \tag{37}$$

where $\hat{v}_1$ and $\hat{v}_2$ are evaluated at $y = 0$. The first of these relations shows clearly that $\hat{v}_j$ is not continuous at the shear boundary. However, the flow normal to the shear interface is continuous and equal to the rate of displacement of the interface in the direction of its normal.

In addition to the above conditions, the admissible perturbations satisfying (32), (33), and (34) will be limited to that class for which

$$D_1 u_1, \quad D_1 v_1, \quad h_1 \to 0, \tag{38}$$

as $y \to -\infty$, and

$$D_2 u_2, \quad D_2 v_2, \quad h_2 \to 0, \tag{39}$$

as $y \to +\infty$. These conditions rule out the possibility of lateral transfer of energy to or from the system, since Dvh must vanish for $|y| \to \infty$ under the above conditions.

6. *Normal Mode Relations.* In lieu of any initial conditions or boundary conditions in respect to $x = \pm\infty$, attention is confined to those normal mode solutions that are of simple harmonic form in x and t. Specifically, the variables $\hat{u}_j$, $\hat{v}_j$, and h_j are considered to be of the form

$$\left.\begin{aligned} \hat{u}_j &= X_j(y)\, e^{i(kx-\sigma t)}, \\ \hat{v}_j &= Y_j(y)\, e^{i(kx-\sigma t)}, \\ h_j &= Z_j(y)\, e^{i(kx-\sigma t)}, \end{aligned}\right\} \tag{40}$$

where k and σ are the wave number and angular frequency, respectively, and X_j, Y_j, and Z_j are complex functions of the real variable y. Thus each of the variables is associated with a common longitudinal wave length $\lambda = 2\pi/k$, wave period $T = 2\pi/\sigma$, and phase-speed $c = \lambda/T = \sigma/k$, but each differs in phase and in respect to variation with y. Regular behavior at $x = \pm\infty$ is assured if k is restricted to real values. Stable solutions are those that have regular behavior for all t (i. e. real σ). It remains to determine the conditions for which stable perturbations satisfying relations (32) to (40) can exist.

Substitution of relations (40) into relations (32) to (34) gives the following relations to be satisfied by the functions X_j, Y_j, and Z_j:

$$-i\omega_j X_j - fY_j + ig'kZ_j = 0, \tag{41}$$

$$-i\omega_j Y_j + fX_j + g'\frac{dZ_j}{dy} = 0, \tag{42}$$

$$i\omega_j Z_j + ikDX_j + \frac{d}{dy}(D_j Y_j) = 0, \tag{43}$$

where

$$\omega_j = \begin{cases} \sigma - kU, & j = 1 \\ \sigma, & j = 2. \end{cases} \tag{44}$$

The y-dependent functions for the two regions are coupled by condition (36), which takes the form

$$i\omega_j(Z_1 - Z_2) + sY_j = 0, \tag{45}$$

where the Y_j and Z_j are evaluated at $y = 0$. Moreover, conditions (38) and (39) require that X_j, Y_j, and Z_j tend to zero for large values of y. The above relations (41) to (45) formally determine the functions X_j, Y_j, and Z_j for given values of the parameters k, g', s, and U, except for an arbitrary constant factor.

The functions X_j and Y_j represent the y-dependent (complex) amplitudes of the longitudinal and transverse perturbations of flow. These can be related directly to Z_j and its derivative by simple algebraic manipulation of relations (41) and (42). The result is

$$X_j = \frac{g'}{(\omega^2_j - f^2)}\left\{\omega_j k Z_j + f\frac{dZ_j}{dy}\right\}, \tag{46}$$

$$Y_j = \frac{-g'i}{(\omega^2_j - f^2)}\left\{fkZ_j + \omega_j\frac{dZ_j}{dy}\right\}. \tag{47}$$

The function $Z_j(y)$ represents the y-dependent amplitude of the perturbation of thickness of the upper layer. If this is real for all y, this would imply that the disturbance of layer thickness is in phase along a line $x = a$ constant at any given t. In other words, the phase lines, transverse to the basic current U, advance in a direction parallel to the basic flow (upstream or downstream, depending on the sign of σ/k). Under these conditions, relations (46) and (47) indicate that X_j is real provided that ω_j is real and that Y_j is imaginary. This implies in turn that the longitudinal perturbation of flow is in phase with Z_j and the transverse flow is $\pi/2$ radians out of phase with Z_j, under the condition that Z_j is real. This is the situation in respect to the solutions investigated in the subsequent sections.

If relations (46) and (47) are employed in (43), the following second order residual equation involving Z_j only is obtained:

$$\frac{d}{dy}\left(D_j\frac{dZ_j}{dy}\right) + (K_j - k^2 D_j)\,Z_j = 0, \tag{48}$$

where

$$K_j = (\omega^2_j - f^2)/g' + (kf/\omega_j)\,(dD_j/dy).$$

Now, since dD_j/dy has the constant value $-s$ for $j = 1$ and 0 for $j = 2$, in the present model, it follows that K_j is simply a parameter independent of y for either region. The only variable coefficient is D_j for $j = 1$. Both K_j and k have the dimensions of reciprocal length.

It remains to find solutions of (48) for each region that satisfy the coupling condition (45) and the restriction $Z_j \to 0$ for large values of y.

Iwata (1961) employed a relation similar to (48) in his analysis of a model of the type dealt with in this paper. Note, however, that his analysis was restricted to the case for which $\omega^2_j \ll f^2$, thus simplifying the expression for K_j. This can be shown to be equivalent to the restriction of quasi-geostrophic perturbations (geostrophic vorticity approximation). This restriction is not imposed in the present analysis.

7. *Formal Solution of the Perturbation Equations.* The solutions of the perturbation equations that are of primary concern are those for which k differs from zero, since these correspond to meanders of finite longitudinal wave length. However, there is one special class of solution with $k = 0$ that should be mentioned before proceeding. This is the class of steady-state solutions for which Z depends upon y alone (hence $\sigma = 0$, $k = 0$). Relations (41) and (42) reveal that $Y_j = 0$ and $X_j = -(g'/f)\, dZ_j/dy$ for this case, since ω_j vanishes for both regions. Moreover, (43) and (45) are satisfied identically for any distribution of Z_j as a function of y. This class of solution is simply a steady geostrophic flow condition superimposed on the basic geostrophically balanced regime. Allowance for a permanent variation in the basic state would be pertinent to situations for which the selected basic state does not correspond to one of stable equilibrium.

The differential equations governing the functions $Z_1(y)$ and $Z_2(y)$ must be treated separately. Using (48) and the pertinent definitions, the particular relations for Z_1 and Z_2 can be expressed as follows:

$$(D_0 - sy)\frac{d^2 Z_1}{dy^2} - s\frac{dZ_1}{dy} + (K - k^2 D_0 + k^2 sy)\, Z_1 = 0, \tag{49}$$

$$\frac{d^2 Z_2}{dy^2} + m^2 Z_2 = 0, \tag{50}$$

where

$$K = \frac{\omega^2 - f^2}{g'} - \frac{fsk}{\omega}, \tag{51}$$

$$m = \left\{\frac{\sigma^2 - f^2}{g' D_0} - k^2\right\}^{1/2}. \tag{52}$$

The first of these differential equations can be brought into a form more comparable to the second by introducing the following transformations:[2]

$$Z_1 = z^{-1/2} G(z), \tag{53}$$

$$z = \frac{2k}{s}(D_0 - sy). \tag{54}$$

The resulting relation, for $G(z)$, is

$$\frac{d^2 G}{dz^2} + N^2 G = 0, \tag{55}$$

where

[2] In the subsequent development, the symbol z is employed exclusively in the sense defined by (54); hence there should be no confusion with the vertical coordinate.

$$N^2 = (2z)^{-2}\left\{1 + (2K/sk)\,z - z^2\right\}. \tag{56}$$

The essential distinction between (50) and (55) is that m^2 is merely a constant parameter while N^2 is a function of the independent variable y.

The general solution of (50) for $m^2 > 0$ (real m) is simply

$$Z_2 = A'_2 \cos my + B'_2 \sin my, \tag{57}$$

and for $m^2 = -M^2$ (M real)

$$Z_2 = A_2 e^{My} + B_2 e^{-My}, \tag{58}$$

where the coefficients are arbitrary constants. Solutions of type (57) or (58) correspond, respectively, to the condition σ^2 greater than or less than $(f^2 + g'D_0k^2)$. The Kelvin boundary wave belongs to the second type.

An examination of the function N^2 reveals that this vanishes for $z = b$, where

$$b = \frac{K}{sk} + \sqrt{1 + \left(\frac{K}{sk}\right)^2}, \tag{59}$$

attention being confined to the domain $z > 0$ (positive D within region 1). For $0 < z < b$, N^2 is positive, while for $z > b$, N^2 is negative. Hence it would be expected that the solution of (55) for a given value of K/sk will display an oscillatory behavior in the range $0 < z < b$ and be of monotonic character for $z > b$. Moreover, if $2kD_0/s$ exceeds b, then the function G, hence Z_1, will be of monotonic character in the meaningful range of z for region 1. Thus the ratio kD_0/sb (or alternatively $k^2 D_0/K$) plays a key role in determining the behavior of $Z_1(y)$ for $y < 0$.

Use of the transformation (53) and the resulting relation (55) is particularly helpful in determining the asymptotic properties of the possible Z_1 functions by employing the W.K.B. method (Morse and Feshback, 1953; Eckart, 1960). On the other hand, the investigation of the general solution of (49) is facilitated by employing the alternative transformation

$$Z_1 = e^{-z/2} F(z). \tag{60}$$

This converts (49) to the standard form of a confluent hypergeometric equation (Rainville, 1952):

$$z\frac{d^2F}{dz^2} + (c - z)\frac{dF}{dz} - \alpha F = 0, \tag{61}$$

in which $c = 1$, and

$$\alpha = \frac{1}{2}\left(1 - \frac{K}{sk}\right). \tag{62}$$

One solution of eq. (61) is the Kummer function $\Phi(\alpha, c; z)$; for $c = 1$ this has the form

$$\Phi(\alpha, 1; z) = 1 + \frac{1}{\Gamma(\alpha)} \sum_{p=1}^{\infty} \frac{1}{(p!)^2} \Gamma(\alpha + p) z^p. \tag{63}$$

A second solution of (61) for $c = 1$, which is linearly independent of $\Phi(\alpha, 1; z)$, is the Tricomi function, $\Psi(\alpha, 1; z)$, defined by

$$\Psi(\alpha, 1; z) = -\frac{1}{\Gamma(\alpha)} \left\{ \Phi(\alpha, z) \ln z + \right.$$
$$\left. + \sum_{p=0}^{\infty} z^p \frac{\Gamma(\alpha + p)}{(p!)^2 \Gamma(\alpha)} [\psi(\alpha + p) - 2\psi(1 + p)] \right\}, \tag{64}$$

where $\psi(\alpha) = d\Gamma(\alpha)/d\alpha$ (Erdelyi *et al.*, 1953). It is apparent that $\Phi = 1$ at $z = 0$, while Ψ has a logarithmic singularity at $z = 0$. For large z, these functions have the following asymptotic behavior:

$$\Phi \to \frac{1}{\Gamma(\alpha)} e^z z^{\alpha - 1},$$
$$\Psi \to z^{-\alpha}. \tag{65}$$

The general solution for Z_1 is

$$Z_1 = A_1 e^{-z/2} \Phi(\alpha, 1; z) + B_1 e^{-z/2} \Psi(\alpha, 1; z). \tag{66}$$

However, in view of the asymptotic behavior for large z, it is apparent that A_1 must be zero if Z_1 is to vanish at large z (large negative y). Likewise, if Z_2 is to vanish for large positive y, then relation (58) with $A_2 = 0$ must be adopted as the admissible solution for region 2. Thus

$$Z_1 = B_1 W(\alpha, z), \tag{67}$$

$$Z_2 = B_2 e^{-My}, \tag{68}$$

where

$$W(\alpha, z) = e^{-z/2} \Psi(\alpha, 1; z). \tag{69}$$

Relation (67) holds for $z \geqslant z_0$ while (68) holds for $y \geqslant 0$, where

$$z_0 = \frac{2kD_0}{s} > 0. \tag{70}$$

The function $W(\alpha, z)$, oscillatory in the range $0 < z < b$ for negative values of α, decays monotonically to zero for $z > b$. If α is a negative integer, then $W(\alpha, z)$ can be represented in terms of the Laguerre function; if $\alpha = \pm(2n + 1)/2$, $W(\alpha, z)$ can be expressed in terms of the modified Bessel function $K_n(z/2)$. These relations and the pertinent recursion relations for

TABLE I. SAMPLE TABULATIONS OF $W(\alpha, z)$.

	$\alpha =$							
z	−4	−3	−2	−1	−0.5	0	0.5	1
0.10	14.4	−4.08	1.53	−.856	−.230	.951	1.76	1.92
0.15	10.2	−3.20	1.32	−.790	−.102	.931	1.54	1.55
0.2	6.84	−2.49	1.122	−.724	.008	.905	1.37	1.35
0.3	1.08	−1.19	.766	−.602	.147	.861	1.15	1.05
0.4	−3.17	−0.14	.459	−.491	.243	.819	.989	.857
0.6	−8.16	1.31	−.0296	−.296	.362	.741	.774	.613
0.8	−9.72	2.11	−.375	−.134	.430	.670	.629	.471
1.0	−9.10	2.42	−.606	0	.468	.607	.521	.360
1.5	−3.28	1.94	−.827	.236	.486	.477	.342	.210
2.0	.2.93	0.73	−.736	.368	.458	.368	.237	.133
3.0	7.37	−1.34	−.223	.446	.355	.223	.1207	.088
4.0	3.24	−1.89	.271	.406	.254	.135	.0643	.0280
6.0	−5.98	−0.30	.696	.249	.117	.0498	.0196	.0072
8.0	−4.25	1.36	.622	.1282	.050	.0183	.0063	.0023
10.0	1.78	1.85	.418	.0606	.0207	.0067	.0021	.0007
15.0	6.31	.89	.1295	.0110	.0014	.0008	.0001	.0000
20.0	2.67	.216	.0146	.0008	.0002	.0000	—	—
30.0	0.134	.006	.0002	—	—	—	—	—

facilitating the evaluation of $W(\alpha, z)$ and its first derivative are given in Appendix A, p. 281. Tables I and II show in tabulated form the behavior of the $W(\alpha, z)$ function.

Again attention must be drawn to the mathematical treatment of the foregoing equations in the work by Iwata (1961). Note the different form in the expression for the Tricomi function in his work, the counterpart of eq. (64) presented here.

8. *The Associated Flow.* Use of relations (46) and (47) with (72) yields the following expressions for the amplitudes of the velocity components associated with a departure from equilibrium:

$$\begin{aligned} Y_1 &= \frac{-ig'kB_1}{(\omega^2 - f^2)}[fW(\alpha, z) - 2\omega W'(\alpha, z)], \\ X_1 &= \frac{g'kB_1}{(\omega^2 - f^2)}[\omega W(\alpha, z) - 2fW'(\alpha, z)], \end{aligned} \tag{71}$$

for region 1, where $W'(\alpha, z)$ denotes the derivative dW/dz. On the other hand, relation (68) yields the following expressions for region 2:

$$\begin{aligned} Y_2 &= \frac{-ig'kB_2}{(\sigma^2 - f^2)}\left[f - \sigma\frac{M}{k}\right]e^{-My}, \\ X_2 &= \frac{g'kB_2}{(\sigma^2 - f^2)}\left[\sigma - f\frac{M}{k}\right]e^{-My}. \end{aligned} \tag{72}$$

TABLE II. ZEROS OF $W(\alpha, z)$ FOR $\alpha < 0$. ENTRIES CORRESPOND TO THE VALUES z_p, FOR WHICH $W(\alpha, z_p) = 0$ FOR THE INDICATED VALUE OF α.* THE LARGEST ROOTS, z_p, ARE ENTERED IN COLUMN 1, THE NEXT LARGEST IN COLUMN 2, ETC.

	$p =$						
α	1	2	3	4	5	6	7
− .5	0.20	—	—	—	—	—	—
−1.0	1.00	—	—	—	—	—	—
−1.5	2.1	.10	—	—	—	—	—
−2.0	3.4	.59	—	—	—	—	—
−2.5	4.7	1.30	.10	—	—	—	—
−3.0	6.3	2.3	.42	—	—	—	—
−3.5	7.8	3.3	.94	.10	—	—	—
−4.0	9.4	4.5	1.72	.32	—	—	—
−4.5	11.0	5.8	2.6	.76	.09	—	—
−5.0	12.7	7.1	3.6	1.42	.27	—	—
−5.5	14.2	8.6	4.6	2.1	.63	.08	—
−6.0	16.0	10.1	5.7	3.0	1.20	.23	—
−6.5	17.7	11.4	6.9	4.0	1.80	.55	.06
−7.0	19.2	12.8	8.2	4.9	2.55	1.03	.20

* Entries of z_p are reliable to about $\pm 2\%$.

It remains to determine the relationship between the constants B_1 and B_2 as well as the relationship between σ, k and the other parameters of the model.

9. *The Characteristic Equation.* The above relations for X_j, Y_j, and Z_j will satisfy the coupling conditions (45) for $j = 1$ and 2 provided that

$$\left\{\omega W(\alpha, z_0) - \frac{g' sk}{(\omega^2 - f^2)}\left[fW(\alpha, z_0) - 2\omega W'(\alpha, z_0)\right]\right\} B_1 = \omega B_2, \tag{73}$$

and

$$\left\{\sigma + \frac{g' sk}{(\sigma^2 - f^2)}\left[f - \sigma\frac{M}{k}\right]\right\} B_2 = \sigma W(\alpha, z_0) B_1. \tag{74}$$

These determine the ratio B_2/B_1 and impose the following characteristic relationship between σ and k:

$$\left\{\omega - \frac{g' sk}{(\omega^2 - f^2)}\left[f - 2\omega\frac{W'(\alpha, z_0)}{W(\alpha, z_0)}\right]\right\}\left\{\sigma + \frac{g' sk}{(\sigma^2 - f^2)}\left[f - \sigma\frac{M}{k}\right]\right\} = \omega\sigma. \tag{75}$$

Recall that

$$\left.\begin{aligned} \omega &= \sigma - kU \\ z_0 &= 2kD_0/s \\ s &= Uf/g', \end{aligned}\right\} \tag{76}$$

while $M^2 = -m^2$ or

$$M = \sqrt{k^2 - \frac{\sigma^2 - f^2}{g' D_0}}, \tag{77}$$

and from (51) and (62)

$$\alpha = \frac{1}{2}\left(1 - \frac{\omega^2 - f^2}{g'sk} + \frac{f}{\omega}\right). \tag{78}$$

Relations (76) and (77) imply that the functions $W(\alpha, z_0)$ and $W'(\alpha, z_0)$ are determined by σ, k and by the model parameters f, g', U, and D_0. Accordingly, the combined relations (75) to (78) imply that

$$\sigma = S_n(k, f, g', U, D_0), \tag{79}$$

the function S_n being multivalued for fixed values of the arguments.

The system of eqs. (75) to (78), which collectively represent the characteristic relationship, can be put into a more convenient form for analysis by introducing the dimensionless variables

$$\gamma = \frac{\omega}{f}, \tag{80a}$$

$$\mu = \frac{Uk}{f} = \frac{g'sk}{f^2} = \frac{F^2 z_0}{2}, \tag{80b}$$

where

$$F = \frac{U}{\sqrt{g' D_0}}. \tag{80c}$$

The parameter γ is a relative "Doppler" frequency, μ is a relative longitudinal wave number, and F is the internal Froude number. The actual frequency σ is simply $(\gamma + \mu)f$. The relative phase-speed is $c/U = 1 + \gamma/\mu$. Thus meanders that are stationary relative to the earth would correspond to the condition $\gamma = -\mu$, while meanders that are carried along with the basic flow would correspond to the condition $\gamma = 0$.

Note that z_0 can be expressed as $2\mu/F^2$. Also, it is not difficult to show that M/k takes the form

$$\frac{M}{k} = \left\{1 - [(\gamma + \mu)^2 - 1]\, F^2/\mu^2\right\}^{1/2}, \tag{81}$$

while α can be expressed as

$$\alpha = \frac{1}{2}\left\{1 - \frac{\gamma^2 - 1}{\mu} + \frac{1}{\gamma}\right\}. \tag{82}$$

Moreover, at the expense of some algebraic manipulations, relation (75) can be rendered in the form

$$\left\{\mu\gamma(CE - 1) + (E - \gamma)(\gamma + \mu)[(\gamma + \mu)^2 - 1]\right\}^2 =$$
$$= [\gamma(\gamma + \mu)(CE - 1)]^2 \left\{\mu^2 - [(\gamma + \mu)^2 - 1]\, F^2\right\}, \tag{83}$$

where

$$C = 2\alpha - 1,$$

$$E(\alpha, z_0) = \frac{W(\alpha, z_0)}{2W'(\alpha, z_0)}. \tag{84}$$

The latter function can be calculated directly for specified values of μ, F, and α, using the identity $z_0 = 2\mu/F^2$.

Formally eqs. (82) and (83) constitute an implicit characteristic relationship for γ in terms of the parameters μ and F alone. However, for each μ and F there exists a countably infinite set of admissible γ. These multiple roots correspond to the different physical classes and to the different geometrical modes in respect to the functions X_j, Y_j, and Z_j. The different γ and the associated functions X_j, Y_j, and Z_j for given μ and F represent the eigen values and eigen functions of the system as controlled by the geometry and inertial aspects of the basic state.

Relation (83) represents an eight-degree polynomial in γ:

$$\sum_{n=0}^{8} A_n \gamma^{8-n} = 0, \tag{85}$$

in which the coefficients A_n depend upon the parameters α, μ, and F. The detailed relations for these coefficients are given in Appendix B (p. 282). Relation (82) can also be expressed in the form of a third degree polynomial in γ:

$$\gamma^3 + [(2\alpha - 1)\mu - 1]\gamma - \mu = 0. \tag{86}$$

In this case the coefficients do not involve F and the roots γ for given α are easily constructed. Graphs of γ versus μ for selected values of α, as determined from (86), are shown in Fig. 4 for negative values of γ. The admissible values of γ (and α) are those that satisfy both (85) and (86) for common μ and F.

The polynomial form of the characteristic equation, (85), was analyzed by computer methods in this work. The coefficients were first found in terms of three values of F^2 (0.1, 1.0, 10.0), 16 values of α, and 30 values of z_0 or rather μ. This produced 1,020 separate polynomials that were then solved for the real roots γ, which were related to the particular F^2, α, and μ that made up the coefficients of each equation. Not all of the roots of (85) are real; moreover, the number of real roots depend on the relative wave length, μ, for given F^2 and α. Graphs of $-\gamma$ versus μ were then constructed, each graph representing 30 of these polynomials. Each graph was divided along its μ axis into mode-number (n) zones. The modal number was determined by the number of zero crossings of the $W(\alpha, z)$ function for z larger than a particular z, or for μ larger than a particular μ. The number of zeros (n)

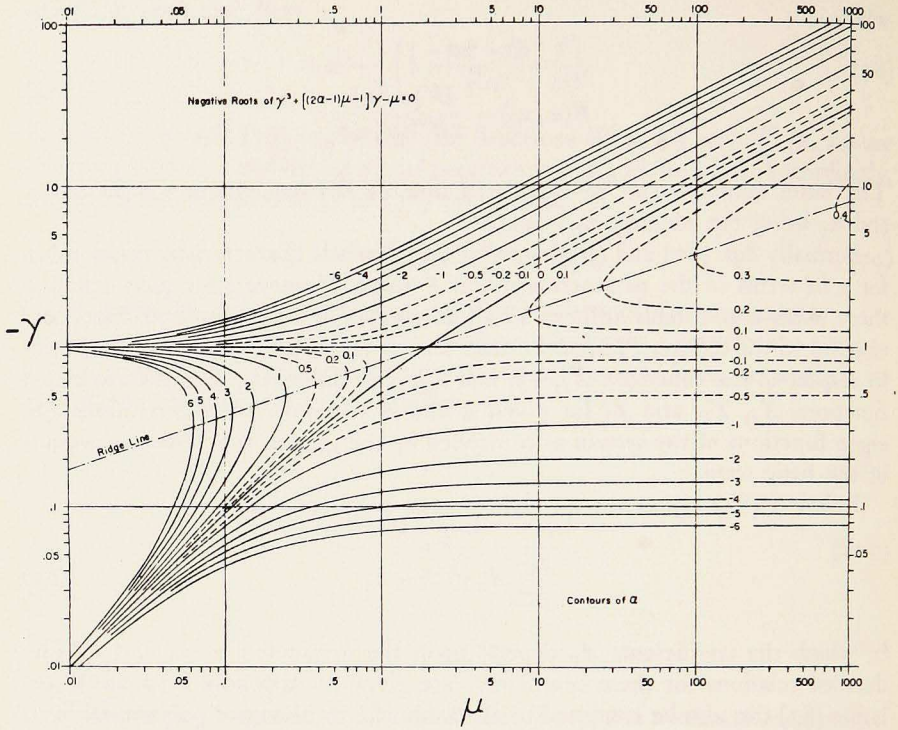

Figure 4. Graph of $-\gamma$ versus μ for different values of the parameter α as evaluated from eq. (86).

correspond literally to a transverse wave number. The 34 graphs obtained in this manner from the polynomial are not included in this article. These graphs were then superimposed on the graphs of eq. (86) (Fig. 4) to determine the admissible values of γ and α for common μ and F. Each point obtained in this manner was labeled with its corresponding modal value n, and contours of n were then drawn to produce the eigen values and functions of the problem. Figs. 5–7 are the results of these manipulations.

10. *Condition Imposed by Real M.* The stipulation of monotonic character of the disturbance in region 2 requires that M be a real number. It is clear from (81) that this is the case if

$$[(\gamma+\mu)^2-1]<\left(\frac{\mu}{F}\right)^2. \tag{87}$$

This condition imposes an upper and lower bound or cut-off on the admissible γ values for given μ and F. Specifically, (87) requires that

$$\gamma_c^-<\gamma<\gamma_c^+, \tag{88}$$

where

$$\gamma_c^{\pm} = \pm \sqrt{\left(\frac{\mu}{F}\right)^2 + 1} - \mu. \tag{89}$$

Values of γ that fall outside the indicated limits would be associated with an oscillatory profile, relation (57), corresponding to the superposition of an in-

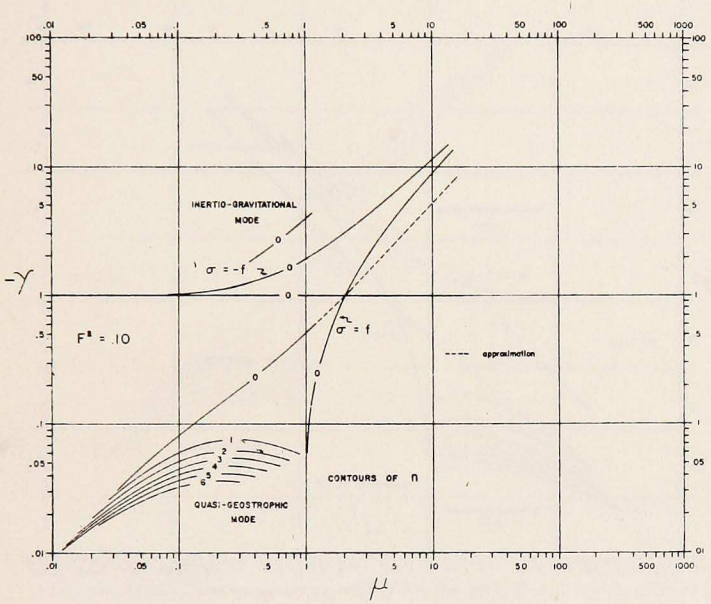

Figure 5. Graph of the admissible negative real values of the relative frequency $\gamma = (\sigma - kU)/f$ versus the relative wave number $\mu = kU/f$ for the case, $F^2 = U^2/g'D_0 = 0.1$. Each curve corresponds to a distinct value of n, which represents the number of zeros of Z in region 1.

cident and reflected wave train in region 2, with wave length $2\pi/\sqrt{k^2+m^2}$, which impinges at an angle $\tan^{-1} m/k$ to the shear boundary.

The curves shown in Figs. 5–7 have been restricted to the range delineated by relation (89).

INTERPRETATION OF THE MODEL

1. *Properties of the Different Wave Modes.* In the interpretation of Figs. 5–7 it is important to bear in mind that γ is a relative frequency of the waves —namely, the frequency apparent to an observer moving with the mean current U in region 1, in a system of units where f has unit value. The angular frequency with respect to a fixed point on the earth is $\sigma = f(\mu + \gamma) = kU + f\gamma$, and the longitudinal wave number is simply $k = (f/U)\mu$.

It is also important to note that while the multiple values of γ versus μ as given in Figs. 5–7 are admissible roots of the pair of relations (85) and (86), all of these roots are not necessarily associated with meaningful disturbances of the system. In particular, $-\gamma = 1$ ($\omega = -f$) is a valid root of the characteristic equations. However, relations (71) indicate that B_1 must vanish if the flow is to remain finite for the case $\omega^2 = f^2$. The roots $\sigma = \pm f$ also

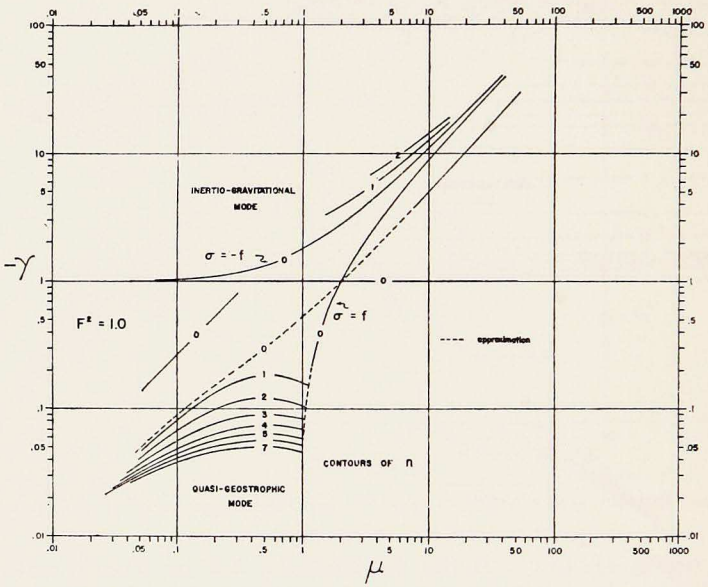

Figure 6. Graph of the admissible negative real values of the relative frequency $\gamma = (\sigma - kU)/f$ versus the relative wave number $\mu = kU/f$ for the case, $F^2 = U^2/g'D_0 = 1.0$. Each curve corresponds to a distinct value of n, which represents the number of zeros of Z in region 1.

emerge from the characteristic equation for $F^2 \leqslant 1$ (Figs. 5 and 6). These correspond to $-\gamma = 1 \pm \mu$. Relations (72) indicate that B_2 must vanish for $\sigma^2 = f^2$ if the flow in region 2 is to remain finite.

In order to obtain determinate solutions for the special cases $\omega^2 = f^2$ and $\sigma^2 = f^2$, it is necessary to return to the basic relations (41) to (45) and set $\omega_j = \pm f$ and $Z_j = 0$ (for $j = 1$ *or* 2). The first two equations lead to the common result $X_j = \pm i Y_j$ (sign to agree with the choice $\omega_j = \pm f$). Relation (43) yields $Y_j = A_j e^{\pm ky}/D_j$, where A_j is a constant. Again the sign corresponds to the choice $\omega_j = \pm f$. Clearly there is only one choice of sign, depending upon the region. For region 1 ($y < 0$), the negative sign is ruled out if the flow is to remain finite at large $|y|$. For region 2 ($y > 0$), the positive sign is ruled out.

This indicates the following situation with regard to the modes in question:

Condition:

$$\omega = +f \begin{cases} Z_1 = 0,\ X_1 = iY_1,\ Y_1 = A_1 e^{ky}/D(y) \\ Z_2 \neq 0, \text{ general solution for region 2,} \end{cases}$$

$$\omega = -f \quad \text{trivial (except for } \mu = 2),^3$$

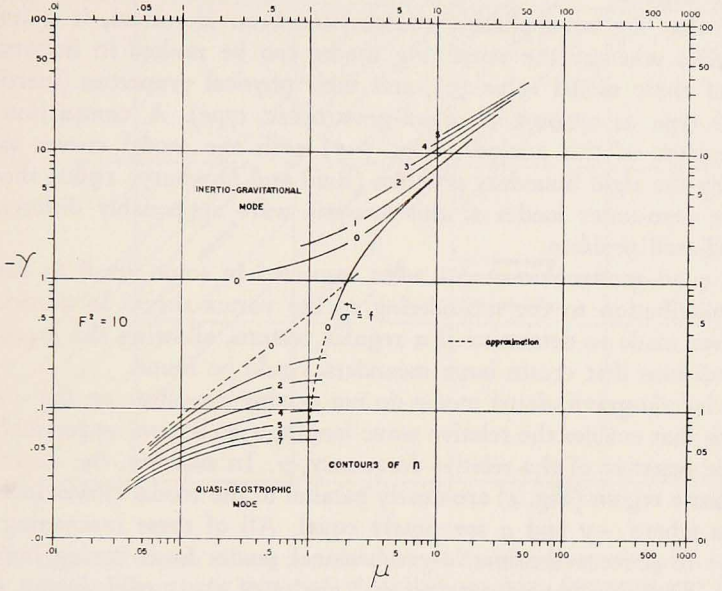

Figure 7. Graph of the admissible negative real values of the relative frequency $\gamma = (\sigma - kU)/f$ versus the relative wave number $\mu = kU/f$ for the case, $F^2 = U^2/g'D_0 = 10.0$. Each curve corresponds to a distinct value of n, which represents the number of zeros of Z in region 1.

$$\sigma = -f \begin{cases} Z_1 \neq 0, \text{ general solution for region 1} \\ Z_2 = 0,\ X_2 = iY_2,\ Y_2 = A_2 e^{-ky}/D_0, \end{cases}$$

$$\sigma = +f \quad \text{trivial (except for } \mu = 2).^3$$

The valid modes $\omega = +f$ ($\sigma = f + kU$) and $\sigma = -f$ indicate that a rotary inertial motion can exist on one side of the shear boundary, with a general disturbance on the other.

Referring to Figs. 5–7 it is apparent that the different wave modes seem to fall into one of two types: those with $|\gamma| > 1$ and those with $|\gamma| < 1$ (corresponding to $|\omega| > f$ or $|\omega| < f$, respectively). As can be seen from relations (46) and (47), the waves with $|\omega| \ll f$ have a nearly geostrophic relation for the flow, while those with $|\omega| \gg f$ have a flow associated with ordinary in-

3 Figs. 5 and 6 indicate a special situation for point $-\gamma = 1$, $\mu = 2$, in which three curves intersect.

ternal gravity waves. Thus the general classification quasi-geostrophic and inertio-gravitational seems appropriate for distinguishing the two classes of wave modes.

An exception occurs for the fundamental zero-order mode. This behaves like the quasi-geostrophic class for small μ and like the inertio-gravitational class for large μ.

Now that the nonapplicable modes have been identified, it is important to establish whether the remaining modes can be ranked in importance in terms of their modal value (n), and their physical properties (inertio-gravitational type as opposed to quasi-geostrophic type). A comparison of the modal curves of this analysis (Figs. 5–7) with the modal curves as determined by the rigid boundary problem (Reid and Duxbury, 1960) shows that only the zero-order modes of this analysis were appreciably different from the rigid-wall problem.

The quasi-geostrophic modes were inspected in some detail to determine their contribution to the meandering of the vortex sheet. In particular, an effort was made to determine if a regular pattern, allowing the prediction of the conditions that create large meanders, could be found.

The inertio-gravitational modes do not occupy a position on the $-\gamma$ versus μ graphs that enables the relative wave length, μ, to become appreciably larger than the negative of the relative frequency, γ. In addition, the curves of $-\alpha$ in the same region (Fig. 4) are nearly parallel to the modal curves intersecting in areas where $-\gamma$ and μ are nearly equal. All of these interacting factors combine to prevent the inertio-gravitational modes from having large wave lengths. Thus the inertio-gravitational modes of the model do not seem to match the meanders as observed in the Gulf Stream. Since the quasi-geostrophic modes have physical characteristics very similar to the waves found in the prototype, they are considered to be the important modes for the meander process. Therefore, the quasi-geostrophic modes appear to be the important meander modes.

Several other features also separate these two physical groupings of wave modes. Fig. 8 shows that all of the inertio-gravitational modes travel upstream against the current, U, and that the quasi-geostrophic modes travel downstream. This in effect requires all frequencies, σ, of the first type to be negative and those of the second type to be positive. This is quite evident from the ratio of c/U for positive U and k. The particular case $F^2 = 10$ (Fig. 7) must be singled out, as the inertio-gravitational modes in this example intersect the $c/U = 0$ curve and thus have both positive and negative values of σ in this region. However, near the line of $\sigma = 0$ ($-\gamma = \mu$), these modes have small wave lengths, $\lambda \to 0$ as $n \to \infty$, and cause only small deflections of the shear boundary. Thus they appear to be insignificant in the meander problem, even though they may be stationary in space as are, approximately, the waves observed on the prototype stream.

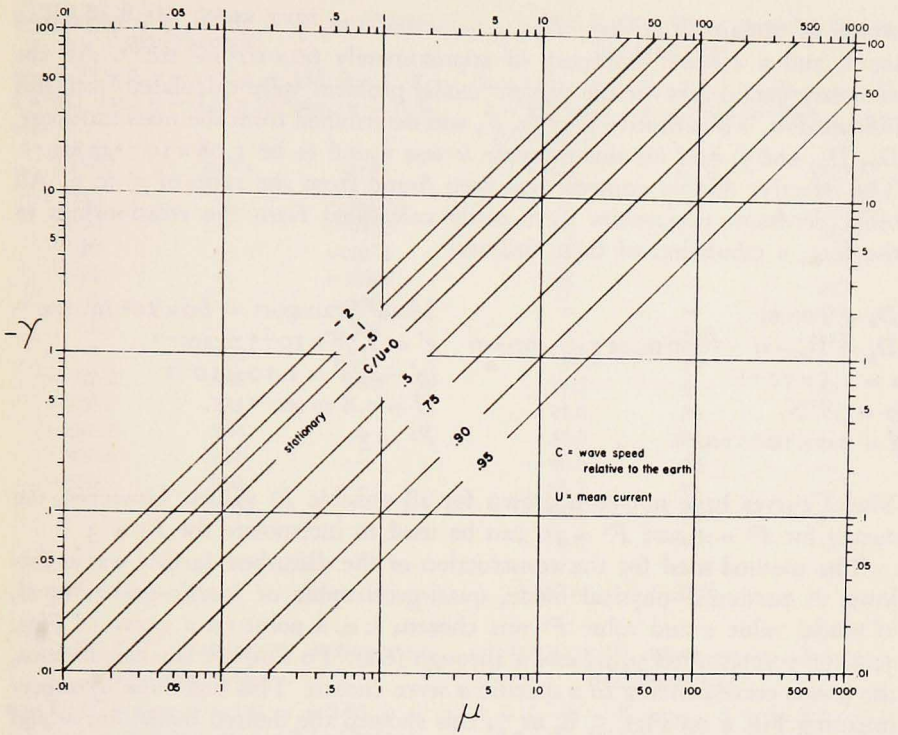

Figure 8. Diagnostic diagram showing contours of the relative phase-speed, c/U, in the γ versus μ diagram. The $-\gamma = \mu$ corresponds to the stationary waves. Comparison with Figs. 5, 6, and 7 reveals that the admissible quasi-geostrophic modes propagate in the same direction as the stream under all conditions of μ and F^2.

2. *Comparison of this Model to the Gulf Stream.* The Gulf Stream has been studied rather intensively in some respects, but most of these studies have provided little information on the transient behavior of the Stream, since data for such studies can be acquired only by expensive multiple-ship surveys over prolonged periods of time. Only one study of time variations, Operation Cabot (Fuglister and Worthington, 1951), has produced the type of information on the Gulf Stream that is requisite for a comparison with the present analysis; it showed that the observed meanders moved downstream at a rate of 18.5 to 20.4 km/day. In addition, it was found that the amplitude of the wave form doubled in approximately two weeks; the wave lengths ranged from 250 to 550 km. The downstream direction of propagation of the waves and the size of the wave lengths indicate that the quasi-geostrophic modes are more apt to be of importance in the meander processes than are the inertio-gravitational modes. From the hydrographic data available for the Gulf Stream, is has been possible to choose reasonable values for the model parameters, such as the physical dimensions of the Stream at a given latitude φ: $D_0 = 100$ m,

width of stream = 60 km, $D_{y=60\,km}$ = 1000 m, $\varphi = 38°N$, $f = 9.0 \times 10^{-5}$ sec^{-1}, and a volume transport of approximately 60×10^6 m^3 sec^{-1}. All the necessary parameters for the present model problem were calculated from this information. The effective gravity, g', was determined from the mass transport, D_0, D_y, and f; and for this example it was found to be 1.08×10^{-2} m sec^{-2}. The effective density contrast was then found from the ratio of g' to g. All other pertinent parameters were easily calculated from the relationships in the text; a tabulation of these follows:

$D_0 = 100$ m	Mass Transport = 60×10^6 m^3 sec^{-1}
$D_y = D_0 - sy = 1000$ m, at $y = -60$ km	$g' = 1.08 \times 10^{-2}$ m sec^{-2}
$s = 1.5 \times 10^{-2}$	$(\varrho' - \varrho)/\varrho' = 1.10 \times 10^{-3}$
$\varphi = 38°N$	$U = 1.8$ m sec^{-1}
$f = 9.0 \times 10^{-5}$ sec^{-1}	$F^2 = 3$

Modal curves have not been drawn for all possible F^2 values. However, the curves for $F^2 = 1$ and $F^2 = 10$ can be used to interpolate for $F^2 = 3$.

The method used for the construction of the disturbed surface was as follows. A particular physical mode, quasi-geostrophic or inertio-gravitational, of modal value n and value F^2 was chosen; i. e. a point on a curve of Figs. 5, 6, or 7 determines γ, μ, and α through (62). To simplify the calculations, the points corresponding to a specific α were chosen. This was done by superimposing Fig. 4 on Figs. 5, 6, or 7; this showed the desired modal curve and determined the γ and μ at the point where the desired α curve intersects the curve $n = a$ constant and $F^2 = a$ constant. Using the values U and f as previously determined, k and z_0 were calculated from (80b) and (76), respectively. Since (54) relates z, z_0, and y, $W(\alpha, z)$ as a function of y was obtained from Table I. Table II was used to determine the zeros of $W(\alpha, z)$ and as a check on z_0, which must be larger than the last z_p [zero crossing of $W(\alpha, z)$ when $n = 0$] and which must lie between the last and the next-to-last zero crossing when $n = 1$. The model parameters and Table I along with Figs. 4–7 were used for the calculation of Z_1 for region 1 (67). Z_2 in region 2 (68) was calculated from (77) and (74), which established the ratio of the constants B_1 and B_2. Therefore, the disturbance in both regions was obtained in terms of the same arbitrary constant B_1. Tables III through VII have been prepared in this manner. Tables III and IV represent cases of quasi-geostrophic modes, and Tables V and VI, inertio-gravitational modes. Table VII differs from Tables III–VI, since the distribution of Z_j with y is not shown; this particular table was constructed to show the effect of the parameters on the excursion, η, of the vortex sheet. Thus calculations of Z_1 and Z_2 were carried out at $y = 0$ only.

The two physical modes in Figs. 5–7 were checked for maximum and minimum values of λ, T, and phase-speed, c. The values obtained for these

TABLE III. WAVE TYPE — QUASI-GEOSTROPHIC

$n = 0$, $F^2 = 3$, $\alpha = -.5$, $\mu = .155$, $\gamma = -.12$, $\lambda = 811$ km, $\sigma = 3.15 \times 10^{-6}$/sec, $\eta = 73.0 \times B_1$

y (km)	z_1/B_1	z_2/B_1
50	—	−.00802
30	—	−.0455
20	—	−.1075
10	—	−.2584
5	—	−.400
1	—	−.566
0	.480	−.617
− 30.2	.486	—
− 126.6	.355	—
− 191.4	.254	—
− 320.8	.117	—
− 450.	.050	—
− 578.	.0207	—

TABLE IV. WAVE TYPE — QUASI-GEOSTROPHIC

$n = 1$, $F^2 = 3$, $\alpha = -1.0$, $\mu = .48$, $\gamma = -.20$, $\lambda = 262$ km, $\sigma = 2.52 \times 10^{-5}$/sec, $\eta = -.333\ B_1$

y (km)	z_1/B_1	z_2/B_1
50	—	−.00764
30	—	−.0430
20	—	−.1018
10	—	−.242
1	—	−.527
0	−.580	−.575
− 3.75	−.40	—
− 14.2	0	—
− 24.6	.24	—
− 35.0	.37	—
− 40.5	.43	—
− 55.7	.45	—
− 66.3	.45	—
− 76.6	.406	—
− 97.4	.249	—
− 182.0	.0606	—

TABLE V. WAVE TYPE — INERTIO-GRAVITATIONAL

$n = 0$, $F^2 = 3$, $\alpha = -1.0$, $\mu = 2.35$, $\gamma = -2.7$, $\lambda = 53.5$ km, $\sigma = -3.1 \times 10^{-5}$/sec, $\eta = 8.8 \times B_1$

y (km)	z_1/B_1	z_2/B_1
30	—	.00176
20	—	.00735
10	—	.0307
1	—	.1112
0	.260	.1285
− 1.85	.368	—
− 3.97	.430	—
− 6.10	.446	—
− 8.24	.450	—
− 10.35	.406	—
− 18.85	.249	—
− 35.9	.0606	—

TABLE VI. WAVE TYPE — INERTIO-GRAVITATIONAL

$n = 1$, $F^2 = 3$, $\alpha = -3$, $\mu = 3.8$, $\gamma = -5.2$, $\lambda = 33.1$ km, $\sigma = -12.6 \times 10^{-5}$/sec, $\eta = 50.5 \times B_1$

y (km)	z_1/B_1	z_2/B_1
20	—	.00395
10	—	.0216
1	—	.100
0	− .64	.1185
− 1.236	− 1.34	—
− 3.87	− 1.89	—
− 9.14	− 0.30	—
− 14.41	1.36	—
− 19.65	1.85	—
− 32.8	.89	—
− 46.0	.216	—
− 72.3	.006	—

TABLE VII. QUASI-GEOSTROPHIC TYPE.

α	n	F^2	μ	$-\gamma$	$\lambda(m)$	z_0	z_1/B_1	z_2/B_1	η/B_1	σ sec^{-1}
−0.5	0	3	.155	.12	811.	1.032	.480	−.617	73.	3.15×10^{-6}
−1.0	1	3	.48	.20	262.	.32	−.580	−.575	−.333	2.52×10^{-5}
−2.0	2	3	.37	.13	339.	.247	.942	.788	10.26	2.16×10^{-5}
−3.0	3	3	.185	.082	679.	.1234	−3.60	115.3	7440.	9.27×10^{-6}
−4.0	4	3	.12	.058	1046.	.080	15.3	19.25	−263.	5.58×10^{-6}

TABLE VIII. LIMITING CHARACTERISTICS OF THE INERTIO-GRAVITATIONAL MODES.

F^2	Mode	λ^*_{min} (km)	λ_o* (km)	λ^*_{max} (km)	Minimum Periods** (hours)		Maximum Phase-Speeds + (km/day)	
					$c>0$	$c<0$	$c>0$	$c<0$
1.0	$n=1$	0	—	84	—	10.8	—	−186.
1.0	$n=2$	0	—	36	—	5.8	—	−145.
10.0	$n=0$	13.4	65.	405	6.25	24.9	+51.4	−390.
10.0	$n=1$	6.68	31.4	144	3.34	19.6	+48.1	−176.5
10.0	$n=2$	4.12	15.5	43.3	1.94	14.9	+50.9	− 69.2
10.0	$n=3$	3.30	10.4	20.6	1.59	10.75	+49.8	− 46.0
10.0	$n=4$	2.85	7.56	14.3	1.38	8.1	+49.6	− 42.4
10.0	$n=5$	2.37	6.28	11.4	1.14	6.46	+49.9	− 42.3

$U = 1.8$ m/sec, $f = 9\times10^{-5}$ sec^{-1} (38°N).
* λ denotes wave length ($\lambda = 2\pi/|k|$); λ_o is that associated with the stationary waves.
** T denotes wave period as observed from a point fixed to the earth ($T = 2\pi/|\sigma|$).
+ Longitudinal phase-speed is positive in the same direction as the basic flow.
− Signifies condition not present.

parameters are tabulated in Tables VIII–X in terms of F^2, modal value n, and physical type. The required model values for the calculation of these tables are the same as those used in computing Tables III–VII.

One case, $F^2 = 10$, is of particular interest, since the modal curves of the inertio-gravitational type of waves intersect the line $-\gamma = \mu$, producing a set of stationary waves. The condition $\sigma = 0$ considerably reduces the characteristic equation for the model and is of some interest. In region 2 the condition $\sigma = 0$ simplifies eq. (45) to $sY_2 = 0$ at $y = 0$. This further requires that $Y_2 = 0$, and then through eq. (72), that $B_2 = 0$. The characteristic eq. (73) may now be simplified to obtain

TABLE IX. LIMITING CHARACTERISTICS FOR THE QUASI-GEOSTROPHIC MODES.

F^2	Mode	λ_{min} (km)	λ_{max} (km)	T_{min}	Maximum $c\,(>0)$ (km/day)
0.1	All n	0		—	—
1.0	All n	0		—	—
10	$n=0$	51.0		15.2	81
10	$n=1$	91		17.2	127
10	$n=2$	98		17.5	135
10	$n=3$	103		17.8	139
10	$n=4$	104		17.5	144
10	$n=5$	106		17.9	141
10	$n=6$	106		17.5	146
10	$n=7$	107		17.5	148

$U = 1.8$ m/sec, $f = 9\times10^{-5}$ sec^{-1} (38°N).
− Undetermined.

TABLE X. LIMITING CHARACTERISTICS FOR THE MONOTONIC WAVES ($n = o$).

F	Class*	λ_{min} (km)	λ_{max} (km)	Minimum Period (hours)		Maximum Phase-Speed (km/day)	
				$c > o$	$c < o$	$c > o$	$c < o$
0.1	(1)	0	—	0	—	78	—
0.1	(2)	—	—	—	19.4	—	155
0.1	(3)	0	125	0	—	155	—
1.0	(1)	0	—	0	—	78	—
1.0	(2)	—	—	—	19.4	—	155
1.0	(3)	0	125	0	—	155	—
10	(1)	51.0	—	15.2	—	81	—
10	(2)	13.4	405	6.25	24.9	51	390
10	(3)	0	125	0	—	155	—

$U = 1.8$ m/sec, $f = 9 \times 10^{-5}$ sec^{-1} (38°N).

* Classification:

(1) Fundamental meander mode; quasi-geostrophic behavior for small μ ($\ll 1$).

(2) Inertial mode for which $\sigma = -f$ for $F^2 \leq 1$ (where $F^2 > 1$, this corresponds to $\sigma = -f$ for $\mu < 1$ only).

(3) Inertial mode for which $\sigma = +f$.

– Undetermined.

$$U + \frac{g's}{k^2U^2 - f^2}\left[f + kU2\,\frac{W'(\alpha, z_0)}{W(\alpha, z_0)}\right] = 0 \tag{90}$$

as the characteristic equation.

Eqs. (78) and (80a, b) may now be modified by $\sigma = 0$ and used jointly to obtain

$$\alpha = \frac{1 - \mu}{2} \tag{91}$$

where

$$\mu = kU/f.$$

Expression (90) can be further reduced with some algebraic manipulation and with the use of (91). The characteristic equation in its final form becomes

$$-2\,\frac{W'(\alpha, z_0)}{W(\alpha, z_0)} = \mu = 1 - 2\alpha, \tag{92}$$

for the case $\sigma = 0$. This is considerably simplified in comparison to the general form, eq. (73). Note that a coupling between regions 1 and 2 is not required for stationary meanders. That is, the shear boundary may have the appearance of a wave fixed in time, but Z_2 is zero whereas Z_1 has considerable latitude in its configuration.

CONCLUSIONS

The simplified model and its analysis as presented here have shown that certain classes of stable waves can exist when the internal Froude number exceeds unity. These stable waves are divisible into two distinct physical classes, inertio-gravitational and quasi-geostrophic modes. These latter modes and the one fundamental mode, common to the quasi-geostrophic modes at small relative frequencies and to the inertio-gravitational modes at large relative frequencies, are the principal modes applicable to the meander problem. Tables VIII–X show clearly that these modes embrace the values of phase speed, wave length, and periods observed in the prototype Stream.

In addition to this physical agreement, it is found that the quasi-geostrophic modes yield large values for η (the displacement of the vortex sheet), when Z_1 and Z_2 are out of phase (see Tables III, IV, and VII). "Large" implies that the ratio of the lateral displacement of the vortex sheet to the change in thickness of the upper layer is much greater than unity. This occurs for wave lengths comparable to those of the Gulf Stream meanders. Under certain conditions, the inertio-gravitational modes also produce a relatively large excursion (Table VI), but this does not correspond to conditions in the Gulf Stream.

The present analysis accordingly supports the notion that the meanders of the real Stream can be treated as quasi-geostrophic disturbances. The analysis does not support previous investigations (Stommel and others) which indicate that disturbances of wave lengths and speeds comparable to those of the real meanders are dynamically unstable when the internal Froude number exceeds unity. The primary influence of the internal Froude number in the present analysis is two-fold: (i) stationary waves are possible on the shear boundary for the relatively short inertio-gravitational modes, and (ii) the range of wave lengths within which shear boundary waves of regular behavior can exist becomes narrower with increasing Froude number. However, this range encompasses, for all F^2, the really significant modes.

The results accordingly shed some doubt on the significance of the internal Froude number as a simple criterion for instability. This is particularly true, since the present model incorporates a velocity discontinuity—a situation that would be expected to enhance the conditions for instability.

At this point, in light of the above findings, it is important to reconsider the model developed by Stommel (1953). The range of applicability of his model as defined by F^2 has already been pointed out. However, there is another important aspect. Stommel assumed that the perturbation terms were independent of y. In order to shed light on the implication of such an approximation, it is partinent to consider the energy balance for the system. A complete energy equation can be formed from (24), (25), and (26) by multiplying by ϱuH, ϱvH, and $\varrho[g'H + 1/2(u^2 + v^2)]$, respectively, and by summing the resulting relations; the following quadratic equation is then obtained:

$$\left.\begin{aligned}&\frac{\partial}{\partial t}\left\{\frac{1}{2}\varrho H(u^2+v^2)+\frac{1}{2}\varrho g'H^2\right\}+\\&+\frac{\partial}{\partial x}\left\{\varrho uH\left[g'H+\frac{1}{2}(u^2+v^2)\right]\right\}+\\&+\frac{\partial}{\partial y}\left\{\varrho vH\left[g'H+\frac{1}{2}(u^2+v^2)\right]\right\}=0.\end{aligned}\right\}\qquad(93)$$

The first quantity set off by braces represents the sum of the kinetic and potential energy of a column of unit cross section extending from the free surface to the bottom. The potential energy $(1/2)\varrho g'H^2$ represents the amount of energy possessed by the two-layer column in excess of that of a reference column of the same mass but of uniform density ϱ'. This energy anomaly is positive provided that $\Delta\varrho$ is positive ($\varrho'>\varrho$), which is clearly the case for a stable density stratification. Moreover, since H can never be negative, it follows that the combined energy density (on a per-unit-area basis) at x, y, and t is positive definite for stable stratification.

The remaining two terms set off by braces in relation (93) represent the x- and y-components of the energy flux through a vertical plane of unit width that extends from the bottom to the free surface. However, all of the energy transport occurs in the upper layer.

Relation (93) has the canonical form of an energy conservation equation for a nondissipative system that is free of any external energy supply. It stipulates that the energy density can change locally only if there is a convergence of the energy flux at the position concerned.

An analogous relation can be obtained from the linear perturbation eq. (32) to (34). If the first of these is multiplied by $\varrho D_j\hat{u}_j$, the second by $\varrho D_j\hat{v}_j$, and the third by $\varrho g'h_j$, and if the resulting relations are added, the following equation is obtained:

$$\left.\begin{aligned}&\frac{\partial}{\partial t}\left\{\frac{1}{2}\varrho D_j(\hat{u}^2{}_j+\hat{v}^2{}_j)+\frac{1}{2}\varrho g'h^2{}_j\right\}\\&+\frac{\partial}{\partial x}\left\{V_j\left[\frac{1}{2}\varrho D_j(\hat{u}^2{}_j+\hat{v}^2{}_j)+\frac{1}{2}\varrho g'h^2{}_j\right]+\varrho g'D_j\hat{u}_jh_j\right\}\\&+\frac{\partial}{\partial y}\left\{\varrho g'D_j\hat{v}_jh_j\right\}=0.\end{aligned}\right\}\qquad(94)$$

The three terms in braces are similar to the three in (93), except that the energy and energy flux now pertain to the perturbations that are superimposed on the basic state.

If Stommel's perturbation equations with their independence of y are handled in the same manner to produce a counterpart of eq. (94), the last

term will appear in the form $-sg'hv$. This means that not only are an energy-density term and an energy-flux term with respect to the x-axis present, but the last term produces energy locally. This local production of energy can in turn produce instability. Thus, the instability found from Stommel's analysis when $F^2 > 1$ may well be a result of the approximations made in the initial formulation of the problem. Professor R. O. Reid pointed out the method by which this discrepancy in Stommel's equations could be detected.

In regard to the amplification of the real meanders of the Gulf Stream, there are three possibilities that could be consistent with the present dynamic model. (i) The actual meanders can be regarded as being composed of a superposition of many quasi-geostrophic modes for a wide band of wave lengths. Also these waves are clearly of dispersive character. Accordingly, a modulated or a localized disturbance on the Stream boundary must undergo changes in form as the disturbance propagates downstream. Some of these disturbances would then grow in amplitude by manner of phase reinforcement. (ii) A second possibility is resonant coupling of the meanders with an external energy source. The torque exerted on the surface by winds would provide a possible coupling mechanism. (iii) A third possibility is that of amplification by virtue of variations of the parameters D_0 and U in the direction of propagation. This could cause an increase in the amplitude analogous to the amplification of swell propagating into shallow water.

In summation, the question of whether or not the actual meanders of the Gulf Stream must be regarded as a true instability, in which the energy of the meanders derives from that of the basic state, remains unresolved. The answer to this question must await more definitive observations that will reveal the dynamic characteristics in greater detail.

REFERENCES

Eckart, Carl
1960. Hydrodynamics of oceans and atmospheres. Pergamon Press, New York. 290 pp.

Erdelyi, A., W. Magnus, F. Oberhettinger, and F. Tricomi
1953. Higher transcendental functions. Bateman Manuscript Project, Vol. 1, McGraw-Hill, New York, pp. 248–292.

Fuglister, F. C., and L. V. Worthington
1951. Some results of a multiple ship survey of the Gulf Stream. Tellus, *3*: 1–14.

Haurwitz, Bernhard, and H. A. Panofsky
1950. Stability and meandering of the Gulf Stream. Trans. Amer. geophys. Un., *31*: 723–731.

Iwata, N.
1961. Über die Instabilität der Meeresströmung in geschiteten Meer. Contr. Mar. Res. Lab., Hydrogr. Off. Japan, *2*(3): 135–170.

Morse, P. M., and H. Feshback
1953. Methods of theoretical physics. McGraw-Hill, New York. 1978 pp.

Rainville, E. D.
1952. Elementary differential equations. Macmillan Co., New York. 449 pp.

Reid, R. O.
1958. Effect of Coriolis Force on edge waves. (I) Investigation of the normal modes. J. Mar. Res., *16*: 109–144.

Reid, R. O., and A. C. Duxbury
1960. The transition from Poincare-Kelvin boundary waves to Stokes type edge waves in a rotating semi-infinite sea. Presented at 41st Annu. Meet. Amer. geophys. Un., April, 1960. Unpublished.

Stommel, Henry
1953. Examples of the possible role of inertia and stratification in the dynamics of the Gulf Stream system. J. Mar. Res., *12*: 184–195.
1958. The Gulf Stream, a physical and dynamical description. Univ. of Calif Press, Berkeley and Los Angeles. 197 pp.

Stommel, Henry, W. S. von Arx, D. Parson, and W. S. Richardson
1953. Rapid aerial survey of Gulf Stream with camera and radiation thermometer. Science, *117*: 639–640.

Appendix A: Properties of the $W(\alpha, z)$ Function

The following are special cases, pertinent recursion relations, and other properties of the function[4]

$$W(\alpha, z) = e^{-z/2}\,\Psi(\alpha, 1, z)$$

expressed in terms of more common functions.

1. *Identities for positive integral values of* α:

$W(0, z) = e^{-z/2}$,
$W(1, z) = e^{-z/2} Ei(-z)$,
$W(2, z) = (z+1)e^{-z/2} Ei(-z) - e^{-z/2}$.

2. *Identities for negative integral values of* α:

$$W(-n, z) = (-1)^n n!\, e^{-z/2} L_n(z),$$

where $L_n(z)$ is the Laguerre polynomial ($n = 1, 2, 3, \ldots$)

$$L_n(z) = 1 - nz + \frac{n(n-1)z^2}{(2!)^2} + \ldots + \frac{(-1)^n}{n!} z^n.$$

3. *Identities for half-integral values of* α:

$$W\left(\frac{1}{2}, z\right) = \frac{1}{\sqrt{\pi}} K_0(z/2),$$

$$W\left(-\frac{1}{2}, z\right) = \frac{1}{2\sqrt{\pi}} [(z-1)K_0(z/2) + zK_1(z/2)],$$

where $K_0(x)$ and $K_1(x)$ are the modified Bessel functions of order 0 and 1, respectively.

4 Notation is that of Erdelyi *et al.* (1953).

4. *Recursion relations*:

$$W(1+n,z) = \frac{1}{n^2}[(z+2n-1)W(n,z) - W(n-1,z)],$$

$$W\left(\frac{n}{2}+1,z\right) = \frac{4}{n^2}\left[(z+n-1)\,W\left(\frac{n}{2},z\right) - W\left(\frac{n}{2}-1,z\right)\right].$$

5. *Derivative relation*:

$$W'(\alpha,z) = \frac{\alpha^2}{z}W(\alpha+1,z) - \left(\frac{1}{2}+\frac{\alpha}{z}\right)W(\alpha,z),$$

or

$$W'(\alpha,z) = \frac{1}{z}\left[\left(\frac{1}{2}z+\alpha-1\right)W(\alpha,z) - W(\alpha-1,z)\right]$$

6. *Asymptotic behavior*:

$$W(\alpha,z) \simeq z^{-\alpha}e^{-z/2}\left[1-\frac{\alpha^2}{z}+\ldots\right]$$

for large z, and

$$W(\alpha,z) \simeq -\frac{1}{\Gamma(\alpha)}[lnz+\psi(\alpha)+1.15443]$$

for small z.

7. *Zeros of* $W(\alpha,z)$:

For $\alpha \geqslant 0$	No zeros of W occur for $z>0$,
$0>\alpha\geqslant -1$	Exactly one zero of W for $z>0$,
$-1>\alpha\geqslant -2$	Exactly two zeros of W for $z>0$,
$-2>\alpha\geqslant -3$	Exactly three zeros of W for $z>0$,
etc.	

The greatest value of z at which $W(\alpha,z)=0$ is less than b, where

$$b = (1-2\alpha)+\sqrt{1+(1-2\alpha)^2},$$

The position $z=b$ corresponds approximately to the point of inflection of W, beyond which the curve is monotonic.

Appendix B: Coefficients of Equation (85)

The coefficients in the relation

$$A_0\gamma^8 + A_1\gamma^7 + A_2\gamma^6 + A_3\gamma^5 + A_4\gamma^4 + A_5\gamma^3 + A_6\gamma^2 + A_7\gamma + A_8 = 0$$

are given on p. 283 in terms of the basic parameters α, μ, and F, with the following abbreviations:

$$C = 2\alpha - 1 \qquad E = W(\alpha, z_0)/2W'(\alpha, z_0)$$
$$L = EC - 1 \qquad z_0 = 2\mu/F^2$$

In this notation the coefficients as derived from (83) are:

$$A_0 = 4\mu^2,$$

$$A_1 = 12\mu^3 - 4\mu^2(C + 2E) + 2\mu F^2 L^2,$$

$$A_2 = 13\mu^4 - \mu^3(10C + 24E) + \mu^2(C^2 + 8CE + 4E^2 + 5F^2L^2 + 4 - 4L - L^2) - \mu(L^2F^2C),$$

$$A_3 = 6\mu^5 - \mu^4(8C + 26E) + \mu^3(2C^2 + 20CE + 12E^2 + 4F^2L^2 + 10 - 6L - 2L^2) - \mu^2[2CL^2F^2 - 2L(C + 2E) + E(8 + 4EC) + C(2 + 2EC)] + \mu(L^2F^2),$$

$$A_4 = \mu^6 - \mu^5(2C + 12E) + \mu^4(C^2 + 16CE + 13E^2 + F^2L^2 + 8 - 2L - L^2) - \mu^3[CF^2L^2 - 2L(C + 3E) + E(20 + 10EC) + C(4 + 4EC)] + \mu^2[1 - 2L + L^2 + 2F^2L^2 + E(4C + 4E + EC^2 - 2LC)],$$

$$A_5 = -\mu^6(2E) + \mu^5[2 + E(4C + 6E)] - \mu^4[C(2 + 8E^2 + 2CE) - 2LE + 16E] + \mu^3[E(8C + 10E + 2EC^2) - 2L(1 + CE) + 2 + L^2F^2] + \mu^2[2E(L - 1 - EC)],$$

$$A_6 = \mu^6(E^2) - \mu^5[E(4 + 2EC)] + \mu^4[1 + 8E^2 + C(4E + E^2C)] + \mu^3[2E(L - 2 - 2EC)] + \mu^2(E^2),$$

$$A_7 = \mu^5(2E^2) - \mu^4[E(2 + 2EC)] + \mu^3(2E^2),$$

$$A_8 = \mu^4(E^2).$$